

Empirical Atomic Sensitivity Factors for Quantitative Analysis by Electron Spectroscopy for Chemical Analysis

C. D. Wagner†

Surfex Company, 29 Starview Drive, Oakland, California 94618, USA

L. E. Davis, M. V. Zeller and J. A. Taylor

Perkin-Elmer Corporation, Physical Electronics Division, 6509 Flying Cloud Drive, Eden Prairie, Minnesota 55344, USA

R. H. Raymond and L. H. Gale

Shell Development Company, P.O. Box 1380, Houston, Texas 77001, USA

Quantitative information from electron spectroscopy for chemical analysis requires the use of suitable atomic sensitivity factors. An empirical set has been developed, based upon data from 135 compounds of 62 elements. Data upon which the factors are based are intensity ratios of spectral lines with F1s as a primary standard, value unity, and K2p_{3/2} as a secondary standard. The data were obtained on two instruments, the Physical Electronics 550 and the Varian IEE-15, two instruments that use electron retardation for scanning, with constant pass energy. The agreement in data from the two instruments on the same compounds is good. How closely the data can apply to instruments with input lens systems is not known. Calculated cross-section data plotted against binding energy on a log-log plot provide curves composed of simple linear segments for the strong lines: 1s, 2p_{3/2}, 3d_{5/2} and 4f_{7/2}. Similarly, the plots for the secondary lines, 2s, 3p_{3/2}, 4d_{5/2} and 5d_{5/2}, are shown to be composed of linear segments. Theoretical sensitivity factors relative to F1s should fall on similar curves, with minor correction for the combined energy dependence of instrumental transmission and mean free path. Experimental intensity ratios relative to F1s were plotted similarly, and best fit curves were calculated using the shapes of the theoretical curves as a guide. The intercepts of these best fit curves with appropriate binding energies provide sensitivity factors for the strong lines and the secondary lines for all of the elements except the rare earths and the first series of transition metals. For these elements the sensitivity factors are lower than expected, and variable, because of multi-electron processes that vary with chemical state. From the data it can be shown that many of the commonly-accepted calculated cross-section data must be significantly in error—as much as 40% in some cases for the strong lines, and far more than that for some of the secondary lines.

INTRODUCTION

Of the techniques useful for analyzing the first few atomic layers of surfaces, ESCA (electron spectroscopy for chemical analysis), known also as XPS (X-ray photoelectron spectroscopy) is the most useful for quantitative analysis. If we assume a solid that is homogeneous to a depth of 10–20 nm (several electron mean free paths), the number of photoelectrons detected per second from an orbital of constituent atoms is given by

$$I = n f \sigma \phi y A T \lambda \quad (1)$$

where n is the number of atoms per cm³ of the element of interest, f is the flux of X-ray photons impinging on the sample, in photons cm⁻² s⁻¹, σ is the photoelectric cross-section for the particular transition in cm² per atom, ϕ is the angular efficiency factor for the instrumental arrangement (angle between photon path and emitted photoelectron that is detected), y is the efficiency of production in the photoelectric process to give photoelectrons of normal energy (with final ionic state the ground state), A is the area of the sample from

which photoelectrons can be detected, T is the efficiency of detection of the photoelectrons emerging from the sample and λ is the mean free path of the photoelectrons in the sample.

In any given accumulation of data on two photoelectrons from a single homogeneous solid

$$\frac{n_1}{n_2} = \frac{I_1 / \sigma_1 \phi_1 y_1 A_1 T_1 \lambda_1}{I_2 / \sigma_2 \phi_2 y_2 A_2 T_2 \lambda_2} \quad (2)$$

If for a given photoelectric transition in an atom in a given sample we let

$$S = \sigma \phi y A T \lambda \quad (3)$$

then

$$\frac{n_1}{n_2} = \frac{I_1 / S_1}{I_2 / S_2} \quad (4)$$

and S is the atomic sensitivity factor discussed in this paper. S is not evaluated for each experimental arrangement but is expressed relative to that of F1s. A recent paper¹ discussed the significant considerations in the applicability of these factors to different samples. Most important is the idea that while the absolute value of S will vary with the matrix because of the variability of

† Author to whom correspondence should be addressed.

the mean free path, λ , the relative values of S will vary only slightly because the ratio λ_1/λ_2 is only slightly matrix-dependent.² With a sample of area large relative to A , from which the electrons are detected, the product AT varies with kinetic energy in a way dictated by the optics of the spectrometer. In the instruments utilized in this study, this relationship is as E^{-1} . The factor y is the only one expected to be significantly matrix-dependent, and that only for elements in paramagnetic forms.

The angular factor ϕ turns out to be not significant with these instruments. The angular dependence of photoelectron emission is given by³

$$dI/d\Omega = I_i/4\pi[1 - \frac{1}{4}\beta(3\cos^2\theta - 1)] \quad (5)$$

where $I_i/4\pi$ is the intensity expected per steradian if the emission were isotropic, θ is the angle between the photon and detected electron, and β is a characteristic parameter for each of the photoelectron interactions, ranging from a low of about 0.8 for some 2p lines to 2.0 for all s lines. The nominal angle, θ , for the Varian instrument is close to 90°, but electrons can be collected at angles from about 85° to 180°, with the most probable angle not far from 90°. That for the PHI instrument ranges from 48° to 132°, with the most probable angle at 50° because of shadowing effects from rough samples.

For the Varian, most of the signal will have $dI/d\Omega = 1.2$ for $\beta = 0.8$ and 1.5 for $\beta = 2.0$. With the PHI, the most probable value is 0.95 for $\beta = 0.8$, ranging up to 1.2, and 0.88 for $\beta = 2.0$, ranging up to 1.5. The most probable variation of ϕ relative to that for s lines in the Varian can be as much as -20% and in the PHI as much as +8%. The variation in the Varian becomes less negative when other angles are considered, and with the PHI the variation becomes less positive, going to a maximum of 20% negative. All variations in ϕ will also be moderated by elastic scattering, which has been shown by Baschenko and Nefedov⁴ to be significant in modifying the expected angular intensities. The conclusion is that the angular effects are below the level expected to be significant, relative to other factors.

Efforts have been made in the past to determine the relative sensitivity factors for the elements, utilizing the strong lines (1s, 2p, 3d and 4f lines). Since peaks for these photoelectrons are of closely similar widths, factors based on peak height are similar. Wagner,⁵ Jørgenson and Berthou,^{6,7} and Nefedov *et al.*^{8,9} published sets of empirically derived factors. These were quoted relative to F1s⁵⁻⁷ and Na1s.^{8,9} Castle and West¹⁰ have published a similar set based upon the use of Si K X-rays.

In all of these studies the number of compounds used was limited, and plots of the data vs. Z gave considerable scatter from smooth monotonic curves. Data from the different authors show considerable disagreement even though most of the data were obtained on instruments of the same manufacture (Varian). Over a period of years we have obtained many more data of use in such calculations, and from two different instruments. Attempts to correlate such experimentally based factors with factors calculated from photoelectric cross-sections, with an energy correction¹¹ gave serious disagreement (30-40% in many cases). It seemed worthwhile to develop an empirically derived set of sensitivity factors resting upon a better statistical base than those attempted heretofore. The data base also

seemed to be adequate to develop a similar set for the next strongest lines in the spectra, termed here secondary lines.

EXPERIMENTAL

IEE-15 (Varian Associates)

Samples were ground in clean alumina mortars in a nitrogen glove box, then dusted on metal cylinders covered with polymer film adhesive tape. The sample was transferred into the instrument without access to air. Data were gathered with either aluminum or magnesium X-rays, generated by a 10 kV 100 ma electron current. Instrumental vacuum was $1-8 \times 10^{-6}$ Torr. Data were obtained at 100 eV pass energy, providing an instrumental line width of 1.0 eV. Sufficient scanning was done to provide peak heights at least 5000 counts above background. Curves were integrated using a baseline drawn tangent to the base at both sides of the peak. This could be done with almost all of the spectra, since complicating shakeup peaks were absent. In the rare cases involving shakeup peaks, e.g. MnF₂, the baseline was drawn to rise in proportion to the integral of the peak at higher kinetic energy, and to merge with the background at the low kinetic energy side of the peak.

PHI 550 (Perkin-Elmer Corporation, Physical Electronics Division)

Data were obtained similarly on this double cylindrical mirror analyzer, using scanning by varying the retarding voltage, and detecting electrons of 100 eV. Operating pressure was $1-5 \times 10^{-8}$ Torr. Samples were ground in air or in a nitrogen-filled glove bag. They were mounted on adhesive tape as above, and transferred into the instrument with minimal air contact. Peak heights were similar to those obtained with the Varian.

Compounds used

As in previous studies, the F1s line is used as the standard, (element 2, Eqn (4)) and sensitivity factors are expressed with F1s as unity. For this purpose, of course, all stoichiometric compounds containing fluorine are useful. While many elements form compounds containing fluorine, there is a large number that do not. For these it is necessary to use a second element as a secondary standard. For this purpose we use potassium, and the K2p doublet. Previous studies have used Na1s as a primary or secondary standard.^{5,8,9} In our experience this was found to lead to difficulties because of the low kinetic energy of the Na1s electrons, compared to most of the photoelectrons that were used, so that results were more sensitive to contamination problems. The energy of the K2p electrons is about median among the photoelectrons used. The average sensitivity factors used for K2p_{3/2} were 0.91 for Mg X-rays and 0.86 for Al X-rays (cf. Table 2).

Compounds used were the purest commercially available. All data accumulated for this and other purposes,

Table 1. Comparison of intensity ratios with the two instruments

Compound	Line	X-rays	KE ratio	Varian	Area ratio, M/F1s PHI 550	Remarks
LiF	Li1s	Mg	2.1	0.023	0.017	
MgF ₂	Mg2p _{3/2}	Mg	2.1	0.067	0.069	
				0.062	0.070	
AlF ₃	Al2p _{3/2}	Mg	2.07	0.12		} Same sample, same laboratory
AlF ₃	Al2p _{3/2}	Al	1.76		0.10	
MgF ₂	Mg2s	Mg	2.05	0.15	0.17	
SrF ₂	Sr3d _{5/2}	Mg	1.97	1.03	1.04	
PbF ₂	Pb4f _{7/2}	Mg	1.96	5.25	5.1	
KAsF ₆	As3d _{5/2}	Al	1.80	0.42	0.40	} Same sample, same laboratory
BaF ₂	Ba4d _{5/2}	Al	1.74	1.04	1.16	
ThF ₄	Th4f _{7/2}	Mg	1.62	7.8	7.55	
KAsF ₆	K2p _{3/2}	Al	1.49	0.85	1.06	} Same sample, same laboratory
BaF ₂	Ba3d _{5/2}	Al	0.88	6.8	8.6	
MgF ₂	Mg1s	Al	0.23	4.36	4.06	
MgF ₂	Mg1s	Al	0.23	3.94		
KAsF ₆	As2p _{3/2}	Al	0.20	7.8	8.1	
BaF ₂	Ba3d _{5/2}	Al	0.51	3.9	4.4	} Same sample, same laboratory
	Ba4d					
	As2p _{3/2}					
KAsF ₆	As3d	Al	0.11	18.5	20.0	

which could supply useful data for this study, were used except those with which independent observations indicated nonstoichiometry, hydrolysis, or presence of other impurities. On this basis, spectra from 13 of the more than one hundred standard samples were rejected.

RESULTS

Compatibility of instruments

It was important to determine whether sensitivity factor data derived from the Varian-IEE and the PHI 550 are comparable before combining them in the statistical treatment. For this purpose, data on fluorides with widely different metallic photoelectron energies were obtained on the two instruments, and are shown in Table 1. With kinetic energy ratios (M/F1s) ranging from 0.2 to 2.0, it was felt that agreement would be adequate verification that the instrumental transmission factors, AT , in the two instruments had identical dependence on kinetic energy. There was no discernible trend with kinetic energy in the differences that exist in Table 1. This indicates also that the carbon contamination under the very different vacuum conditions in the two instruments was not a significant factor in affecting the intensity ratios.

In these instruments, where sweeping the energy range is done by varying the retarding voltage, S is only slightly dependent upon kinetic energy, because $AT\lambda$ varies with E^{-1} † and λ varies as about $E^{0.66}$.² (In Eqn (1) the product AT is about $E^{-0.34}$.) In other instruments with scanning by changing voltages on the analyzer hemispheres or sectors, the detection efficiency

† Seah¹² has pointed out that this relation in the Varian instrument should become E^{-2} below kinetic energies of about 6 E_p or 600 eV. The agreement with such low energy lines as Mg1s (182 eV) and As2p_{3/2} (164 eV) does not seem consistent with this in these experiments.

varies as E^{+1} and the overall dependence ($AT\lambda$) becomes $E^{1.66}$. With instruments with slits and electron lens sections, the energy dependence becomes more complex.^{10,13} Therefore it is not clear that the data herein can be utilized without modification in instruments other than the types used in this study.

Data on area ratios

Experimental data on area ratios of the strong lines are shown in Table 2. Data acquired near the same time with the same sample on the same instrument were averaged and are indicated as single points. Data acquired at widely separated times on the same compound (not necessarily the same sample) on the same instrument were averaged and are so indicated in Table 2 by the superscript 'm'. Data acquired with different X-rays or different instruments are listed in the Table as separate entries. Included are points from references 5, 8 and 14. A few data are included with C1s as the secondary standard, with C1s taken as 0.25. Six points are included from a study by Evans, Pritchard and Thomas,¹⁴ using an instrument with different transmission function. Their data were used where kinetic energy differences in the two lines were small, so that the theoretical energy correction, $(E_1/E_2)^{-2}$ was minimal, ranging from 0.75 to 1.25. This correction was made to their data, on the assumption that intensity in their instrument varies as $E^{1.66}$.

These data include experiments performed with both Mg and Al radiation. It is of interest to determine whether they should be treated separately. Examination of the data on the strong lines show no preponderance of high or low values when either radiation is used on the same compound, except in the 4f series where data with Mg X-rays seem clearly to lead to larger sensitivity factors. The ratios of the photoelectric cross-sections relative to F1s¹⁵ are very similar for Mg and

Table 2. Data base for strong line sensitivity factors

Line	Element	Compound	X-rays		Line	Element	Compound	X-rays	
			Mg	Al				Mg	Al
1s	Li	LiF	0.023	0.022 ⁵	2p _{3/2}				
			0.017	0.019 ⁸			K ₂ NbF ₇	0.96	0.98
	Be	BeF ₂		0.040 ⁸			KSbF ₆	0.83	0.69 ⁵
	B	NaBF ₄	0.103 ^m	0.14 ⁵			K ₂ TaF ₇	0.96	0.89
		KBF ₄	(K) ^d 0.136 ¹⁴						
	C	(CF ₂) _n	0.24	0.24 ⁵				K average	0.91
				0.24 ⁸				± 0.09	± 0.11
	N	(NH ₄) ₃ AlF ₆	0.40			Ca	CaF ₂	0.92	0.96
		(NH ₄) ₃ InF ₆		0.42			CaCO ₃	(C)	1.01 ⁵
		KNO ₃	0.50	0.49		Sc			0.88
		KSCN	0.43 ¹⁴			Ti	K ₂ TiF ₆	1.14	0.98
		K ₂ Hg(SCN) ₄		0.42				(K)1.15	1.10 ⁵
		CO(NH ₂) ₂	(C) ^c	0.43 ⁸		V			
	O	AgOCCF ₃		0.65		Cr	K ₂ CrO ₄		1.46
		KNO ₃	0.67	0.70			K ₂ Cr ₂ O ₇		1.75
		K ₂ SO ₄	0.66	0.70		Mn	MnF ₂	2.01	1.66
		KClO ₃	0.74			Fe	K ₃ FeF ₆	1.82	2.05
		K ₂ MoO ₄		0.69				(K)2.05	2.57
		K ₂ WO ₄	0.71			Co			
		Na ₂ CO ₃	(C)	0.60		Ni	NiF ₂	2.91	
		CaCO ₃	(C)	0.76 ^m		Cu	CuF ₂	4.0	4.5 ^m
		PbCO ₃	(C)	0.60		Zn	ZnF ₂	5.15	6.65
		C ₅ H(COOH) ₄ ^{b)}	(C)	0.76					4.25 ⁵
	Na	NaF	1.57	2.06 ^m		Ga			
			2.24 ¹⁶	1.88 ⁸		Ge	Na ₂ GeF ₆		4.1
		NaBF ₄	2.57	2.59 ⁵					5.6 ⁵
			3.43 ¹⁶			As	KAsF ₆		6.9 ^m
		Na ₃ AlF ₆	1.84 ^m						8.1
		Na ₂ SiF ₆	1.98	2.20 ^m		Ge	Na ₂ GeF ₆	0.19	0.26
			2.26 ¹⁶	1.88 ⁸		As	KAsF ₆		0.24
		Na ₂ TiF ₆	2.31					(K)	0.24
		Na ₂ GeF ₆	1.80	2.19 ^m					0.26
			2.70 ¹⁶			Se			
		Na ₂ ZrF ₆	1.67	1.98 ^m		Br	KBr	0.51	0.53
		NaSnF ₃		2.06 ^m				0.56	0.56
1s	Mg	MgF ₂		4.15 ^m	2p _{3/2}	Rb			
				4.06		Sr	SrF ₂	1.03	0.80
			0.064 ^m	0.051 ^m				1.04	1.03 ⁵
			0.069 ^m	0.066 ^m		Y	YF ₃	1.52	1.22
	Al	AlF ₃	0.12	0.10		Zr	Na ₂ ZrF ₆	1.39	1.03 ^m
		(NH ₄) ₃ AlF ₆	0.13			Nb	K ₂ NbF ₇	1.60	1.67
		Na ₃ AlF ₆	0.11					(K)1.56	1.33
	Si	Na ₂ SiF ₆	0.18	0.17 ⁵		Mo	K ₂ MoO ₄		1.42
		CoSiF ₆	0.24				K ₄ Mo(CN) ₈		1.17
		NiSiF ₆	0.23				K ₃ Mo(CO)(CN) ₃		1.41
		K ₂ SiF ₆	0.19 ¹⁴						
	P	AgPF ₆		0.24		3d _{5/2}	Ru		
	S	K ₂ SO ₄	0.40	0.30		Rh	K ₃ RhCl ₆ · 3H ₂ O		2.64
			0.33 ¹⁴			Pd	K ₂ PdCl ₄	1.94	1.99 ^m
		KNDS ^{a)}		0.36		Ag	AgOCCF ₃		3.8
		K ₂ Hg(SCN) ₄		0.27			AgPF ₆		4.2
		KSCN	0.33 ¹⁴			Cd	CdF ₂	4.45	3.85
	Cl	KCl	0.49	0.49					3.8 ⁵
			0.46 ¹⁴			In	InF ₃	5.3	4.7
		KClO ₃	0.51	0.44			(NH ₄) ₃ InF ₆		4.45
		KClO ₄		0.47		Sn	NaSnF ₃		4.15
		K ₃ RhCl ₆ · 3H ₂ O		0.49					5.8 ⁵
		K ₂ PdCl ₄	0.43	0.41 ^m		Sb	KSbF ₆	5.9	6.7 ⁵
		K ₂ PtCl ₄	0.46 ^m					(K)5.7	
	K	KF	1.03	0.88		Te			
				0.94 ⁵		I	KI	4.8	
		K ₂ TiF ₆	0.85	0.75		Xe			
				0.88 ⁵		Cs			
		K ₃ FeF ₆	0.81	0.72		Ba	BaF ₂	5.8	6.8 ^m
		KAsF ₆		0.88 ^m					

Table 2 (continued)

Line	Element	Compound	X-rays		Line	Element	Compound	X-rays	
			Mg	Al				Mg	Al
			7.0	8.6 6.6 ⁵		Re	KReO ₄	1.96	1.77 ⁵
	La	LaF ₃	5.6			Os			
	Ce					Ir			
	Pr	PrF ₃	5.15			Pt	K ₂ PtCl ₄	2.62 ^m	2.11
	Nd	NdF ₃	4.35				K ₂ Pt(CN) ₄		1.93
	Pm					Au			
	Sm	SmF ₃	3.0			Hg	K ₂ Hg(SCN) ₄		3.9
	(Eu, Gd, Tb, Dy, Ho, Er, Tm, Yb, Lu)					Tl			
4f _{7/2}	Hf	HfF ₄	1.49	0.82	4f _{7/2}	Pb	PbF ₂	5.25	4.5
				0.85 ⁵				5.1	4.1 ⁵
	Ta	K ₂ TaF ₇	1.69	1.51		Bi			
		(K)1.65		1.42		Th	ThF ₄	7.8	6.5
	W	K ₂ WO ₄ · 2H ₂ O	1.51					7.55	
						U	UO ₂ F ₂		6.45 ⁵

^a K salt of 2-naphthol-6, 8-disulfonic acid.

^b Cyclopentanetetracarboxylic acid.

^c C1s used as a secondary standard = 0.25.

^d K used as a secondary standard = 0.91 with Mg X-rays, 0.86 with Al X-rays.

^m Mean of two or more values, run on same compound (not necessarily same sample) at widely different times on same instrument.

⁵ Ref. 5.

⁸ Ref. 8, taking factor for Na1s = 1.88.

¹⁴ Ref. 14, from relative line areas, with energy correction (see text).

¹⁶ Ref. 16.

Al X-rays, with values of the ratio averaging only several per cent larger with Mg (7% in the 3d and 4f series).

Reproducibility of particular line area ratios for the same compound and for different compounds is covered rather exhaustively in an earlier publication.¹ Standard deviation in the ratio for a line pair of similar kinetic energy was 7% when comparing reproducibility for the same compound and 10% for the line pair from different compounds. Swingle¹⁶ provides evidence that variations in y among compounds are responsible. Variations become extreme with paramagnetic species, and with these the line intensities are significantly depressed. Variability is also increased when lines of widely different kinetic energies are compared, because of the effects of variable surface contamination (see below).

Theoretical sensitivity factors for the strong lines

Carter, Schweitzer and Carlson¹⁷ were the first to propose a theoretically derived set of sensitivity factors. From the relation for relative sensitivity factors based upon Eqn (3) they in effect assumed ϕ_1/ϕ_2 and y_1/y_2 to be unity, AT independent of E , and λ proportional to E^{+2} , so that $S_1/S_2 = \sigma_1/\sigma_2(\lambda_1/\lambda_2)^{1/2}$. Many workers use the set of theoretically derived cross-sections alone as sensitivity factors because the values are monotonic relations with Z and their use with some instruments is attended with only small error. Efforts to use the empirically derived factors presented thus far have been hampered by the lack of statistical smoothing of the many data.

The cross-sections calculated by Scofield¹⁵ by the Hartree-Fock-Slater method can be presented usefully on a log-log plot against binding energy.¹⁴ (Similar calculations of cross-sections have been presented by Nefedov *et al.*^{8,9}.) For the binding energies in the following we use the mid-point in the binding energy range for an element with different chemical states.¹¹ When this is done for the 1s interaction with Al X-rays the curve becomes a straight line, Li-Ne, with correlation coefficient of 0.9999, as shown in Fig. 1. That for Mg X-rays is of slightly higher magnitude, and the curves for Mg and Al cross, as shown. Above neon the curves form straight line segments of slightly lower slope. The 2p_{3/2} curve is almost straight, with correlation coefficient 0.9998, from Si to Ga. Values of σ/σ_{F1s} for Ge and As fall about 5% below those that would fit the log-log straight line plot. The segment Mg-Si seems to fit a straight line of lower slope.

The 3d_{5/2} curve is more complex. Most of it fits two straight lines of different slope, one As-Zr, correlation coefficient 0.9993, the other Zr-Dy, correlation coefficient 0.9997. The segment Ga-As has the lowest slope, As-Zr the next, and Zr-Dy the highest. A similar pattern is observed with the 4f_{7/2} transition (Fig. 1). There are three line segments, of increasing slope, Hf-Re, Re-Ra (correlation coefficient 0.9998) and Ra-Am. The curves for Mg X-rays have slightly lower slope in all cases, nearly coinciding at high binding energies and, at low binding energies, diverging to 6% (1s) and to 15% (2p and 3d) higher values than those for Al X-rays. The absolute values of cross-sections for Mg and Al radiation for F1s, the base, differ by 4%.

These cross-sections have been used to calculate atomic sensitivity factors by the following reasoning:¹¹ The quantity AT should vary as E^{-1} theoretically, and,

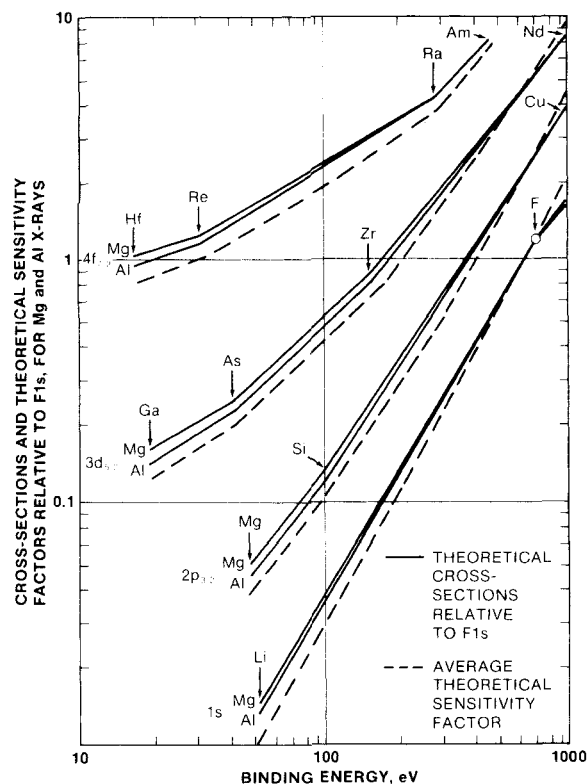


Figure 1. Photoelectric cross-sections of the strong lines, plotted against binding energy of the transitions; derived theoretical sensitivity factors.

indeed, experimental data were obtained that support this: with these instruments the counting rate should be dependent upon electron kinetic energy and pass energy in the following way¹⁸

$$I = \frac{C}{E} E_p^2 \quad (6)$$

where E is the electron energy and E_p is the pass energy. A test of this relationship on the PHI 550 with a copper specimen in continuum parts of the spectrum between 254 and 1050 eV kinetic energy gave counting rates exactly dependent upon the pass energy squared, with pass energies 25 eV–200 eV (cf. Fig. 2).

The relationship between λ and E is rather more difficult to ascertain. The theoretical relation is not simple,¹⁹ but there is little error if one assumes the approximate simple exponential $\lambda = aE^m$. The data that

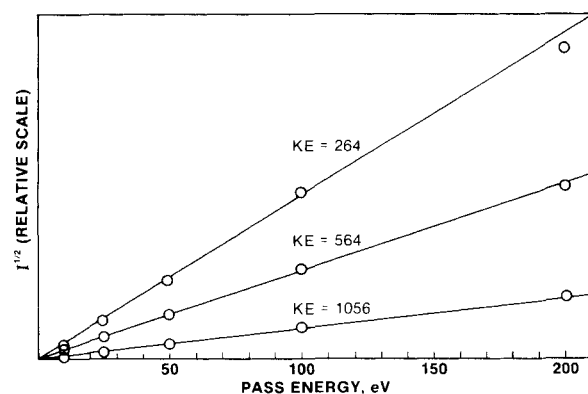


Figure 2. Test of the transmission characteristics of the PHI 550 instrument; the square root of the background intensity versus the pass energy, for copper.

Penn²⁰ calculated provide an exponent m between 0.68 and 0.82. Experimental multi-point data on nine materials provide least squares fit with m in the range 0.54–0.81, averaging 0.66.² If we assume as an approximation that ϕ_1/ϕ_2 and y_1/y_2 are unity, the relative sensitivity factors are then given by

$$\frac{S_1}{S_2} = \frac{\sigma_1}{\sigma_2} \left(\frac{E_1}{E_2} \right)^{-0.34} \quad (7)$$

The energy correction term used in Ref. 11 was $(E_1/E_2)^{-0.25}$, based upon the apparent average value of the exponent from Penn's calculations. In Fig. 1 are plotted calculated curves on the basis of $(E_1/E_2)^{-0.34}$. These are average curves for both Mg and Al radiation. Since the cross-section curve for Mg X-rays represents larger values than those for Al, and since the energy correction for Mg X-rays is larger, the energy corrected curves for the two radiations more closely coincide. For binding energies below about 900 eV, the maximum difference is less than 9%.

Empirical area sensitivity factors for the strong lines

The data in Table 2 have been entered in Figs 3–6. In generating best fit curves to these empirical sensitivity factor data, it has been assumed that their form should be the same as that of the calculated sensitivity factors (shown in Fig. 1, dashed curve), but that the overall slopes and magnitudes might differ. The following describes the details: equations for the following line

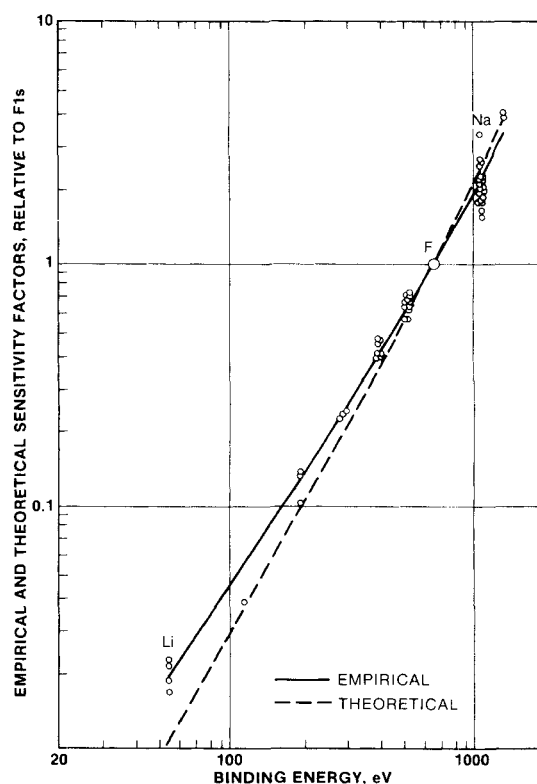


Figure 3. Empirical sensitivity factors for 1s transitions, compared to theoretical sensitivity factors.

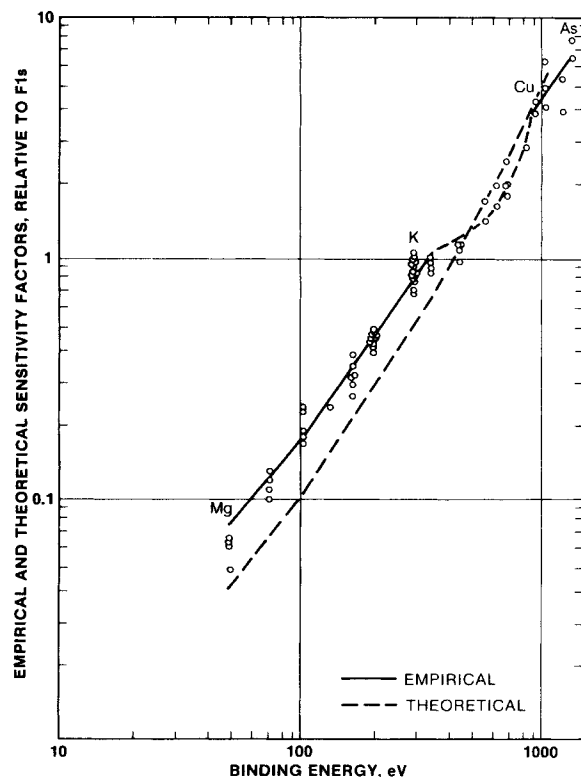


Figure 4. Empirical sensitivity factors for $2p_{3/2}$ transitions.

segments were derived from theoretical sensitivity factors by a best linear fit procedure:

Line	Elements	Correlation coefficient
1s	Li-F	1.000
$2p_{3/2}$	Si-Ca	0.9998
$3d_{5/2}$	As-Zr	0.999
	Zr-Ba	1.000
$4f_{7/2}$	Re-Bi	0.998

No effort was made to include the transition elements, Sc-Ni, because the empirical values for these elements clearly cannot be treated in this manner (Fig. 4). The

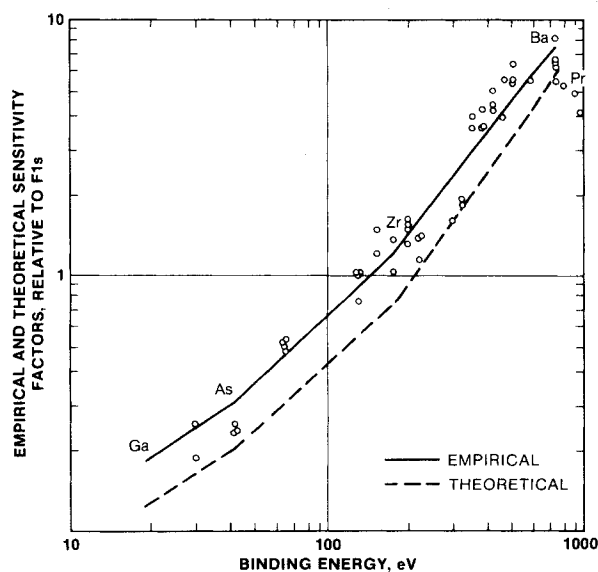


Figure 5. Empirical sensitivity factors for $3d_{5/2}$ transitions.

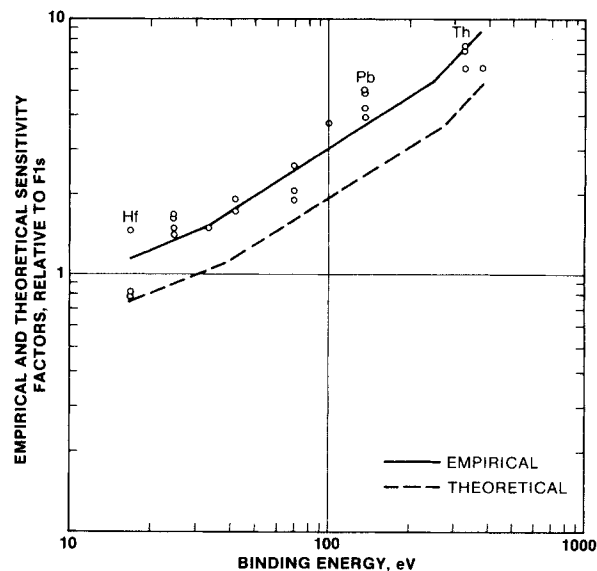


Figure 6. Empirical sensitivity factors for $4f_{7/2}$ transitions.

intensities from these photoelectron transitions are too low, because of significantly reduced values of γ . This leaves the segment of the $2p$ curve, Cu-As, to be treated separately. The rare earths, La-Gd, are also omitted from the $3d$ curve (Fig. 5) for similar reasons.

Deviations of the theoretical $\ln S$ from the extrapolated straight line segments were calculated for (1s) Li-Na, (2p) Mg-Ca, (3d) Ga-Zr and Zr-Ba, and (4f) Hf-U. These deviations were subtracted from each of the experimental points ($\ln S$ of Table 2). The corrected $\ln S$ were fitted to best fit straight lines for the above extended segments. Intercepts for each elemental $\ln BE$ were calculated from the resulting equations, the deviation $\Delta \ln S$ added back, and anti- $\ln S$ values calculated to give the curves in Figs 3-6 and values in Table 3.

A minor adjustment was required in the $3d$ curve. Independent generation of two sets of data with a common point at zirconium led to a 15% discrepancy in that value. Since the lower BE segment had significantly fewer data points, the slope of the curve was reduced to bring the zirconium data into agreement, raising the values at the low end for Ga-As by 10-15% and leaving those for Se-Rb essentially unchanged.

Values for high binding energy points are more difficult to assign because variability due to contamination can become serious for low kinetic energy electrons (see below). With Mg1s the experimental points fit rather close to a linear extension of the curve, and the value of 3.5 was assumed. For Cu-As a best fit straight line was calculated for the empirical data for those elements alone. The slope was reduced very slightly to extrapolate to the Mg-Ca curve and the intercepts then used for Table 3. These data are slightly lower than the extrapolated Mg-Ca curve, and lower than the theoretical curve. Values for the transition metals were interpolated in a smooth fit to the experimental data, but the intercepts recorded in Table 3 are indicated as being only approximate, since the data will be variable with chemical state. Data for the rare earths are also roughly based upon very few experimental points, and the data indicated are only a rough approximation. Area sensitivity factors for unresolved spin doublets are calculated

Table 3. Empirically derived atomic sensitivity factors (Relative to F1s = 1.00)

	Strong line		Secondary line ^b	
	Area	Height ^a	Area	Height
	1s	1s	2s	2s
Li	0.020	0.020		
Be	0.059	0.059		
B	0.13	0.13		
C	0.25	0.25		
N	0.42	0.42		
O	0.66	0.66	0.025	0.025
F	1.00	1.00	0.04	0.04
Ne	1.5	1.5	0.07	0.07
Na	2.3	2.3	0.13	0.12
Mg	3.5 ^{*c}	3.3 [*]	0.20	0.15
	2p _{3/2}	2p		
Mg		0.12	0.20	0.15
Al		0.185	0.23	0.17
Si		0.27	0.26	0.19
P		0.39	0.29	0.21
S		0.54	0.33	0.24
Cl		0.73	0.37	0.25
Ar		0.96	0.40	0.26
K	0.83	1.24	0.43	0.26
Ca	1.05	1.58	0.47	0.26
Sc	(1.1)	(1.65)	0.50	0.26
Ti	(1.2)	(1.8)	0.54	0.26
			3p	3p
Ti	(1.2) ^d	(1.8)	0.21	0.15
V	(1.3)	(1.95)	0.21	0.16
Cr	(1.5)	(2.3)	(0.21)	(0.17)
Mn	(1.7)	(2.6)	(0.22)	(0.19)
Fe	(2.0)	(3.0)	(0.26)	(0.21)
Co	(2.5)	(3.8)	(0.35)	(0.25)
Ni	(3.0)	(4.5)	(0.5)	(0.3)
Cu	(4.2)	(6.3)	(0.65)	(0.4)
Zn	4.8	4.8	0.75	0.40
Ga	5.4	5.4	0.84	0.40
Ge	6.1 [*]	6.0 [*]	0.92	0.40
As	6.8 [*]	6.8 [*]	1.00	0.43
	Area	Height	Area	Height
	3d _{5/2}	3d	3p _{3/2}	3p
Ga		0.31		0.84
Ge		0.38		0.91
As		0.53		0.97
Se		0.67		1.05
Br		0.83		1.14
Kr		1.02	0.82	1.23 ^e
Rb		1.23	0.87	1.30
Sr		1.48	0.92	1.38
Y		1.76	0.98	1.47
Zr		2.1	1.04	1.56
Nb	1.44	2.4	1.10	0.72
Mo	1.66	2.75	1.17	0.73
Tc	1.89	3.15	1.24	0.73
Ru	2.15	3.6	1.30	0.73
Rh	2.4	4.1	1.38	0.74
Pd	2.7	4.6	1.43	0.74
Ag	3.1	5.2	1.52	0.75
Cd	3.5		1.60	0.75
In	3.9		1.68	0.75
Sn	4.3		1.77	0.75

Table 3 (continued)

	Strong line		Secondary line ^b	
	Area	Height ^a	Area	Height
Sb	4.8	4.8	4d	4d
Te	5.4	5.4	1.00	0.86
I	6.0	6.0	1.23	0.97
Xe	6.6	6.6	1.44	1.08
Cs	7.2	7.0	1.72	1.16
Ba	7.9	7.5	2.0	1.25
La	(10) ^d		2.35	1.35
Ce	(10)		(2)	
Pr	(9)		(2)	
Nd	(7)		(2)	
Pm	(6)		(2)	
Sm	(5)		(2)	
Eu	(5)		(2)	
Gd	(3)*		(2)	
Tb	(3)*		(2)	
		4d		4p _{3/2}
Dy		(2) ^d		(0.6) ^d
Ho		(2)		(0.6)
Er		(2)		(0.6)
Tm		(2)		(0.6)
Yb		(2)		(0.6)
Lu		(2)		(0.6)
Hf	4f _{7/2}	Area	4f	Height
			2.05	1.70
Ta			2.4	1.89
W			2.75	2.0
Re			3.1	2.1
Os			3.5	2.2
Ir	2.25	3.95	2.4	1.84
Pt	2.55	4.4	2.55	1.92
Au	2.8	4.95	2.8	2.05
Hg	3.15	5.5	3.15	2.15
	Area	Height	Area	Height
	4f _{7/2}	4f	4d _{5/2}	4d
Ti	3.5	6.15	2.25	0.95
Pb	3.85	6.7	2.35	1.00
Bi	4.25	7.4	2.5	1.00
Th	7.8	7.8	3.5	1.2
U	9.0	9.0	3.85	1.3
	Area	Height	Area	Height
	4f _{7/2}	4f	5d _{5/2}	5d
Ti	3.5	6.15	2.25	0.95
Pb	3.85	6.7	2.35	1.00
Bi	4.25	7.4	2.5	1.00
Th	7.8	7.8	3.5	1.2
U	9.0	9.0	3.85	1.3

^a Height sensitivity factors based on line widths for strong lines of 3.1 eV, typical of lines obtained in survey spectra on insulating samples. When spin doublets are unresolved, data are for the convoluted peak height.

^b Factors for the strong lines are insensitive to the radiation source (Mg or Al). Factors for the secondary lines (2s, 3p, 4d and 5d) are dependent to an extent upon the photon energy. Values shown are average for Al and Mg. For more accurate results, multiply the factors by 0.9 when Mg radiation is used, and by 1.1 when Al radiation is used.

^c Starred data are for peaks obtained only by using Al X-rays.

^d Data in parentheses indicate great variability with chemical state, because of the prevalence of multi-electron processes. Data shown for the series Ti-Cu are for diamagnetic forms; data for paramagnetic forms will be lower in general. Data for the rare earths are based on few experimental points, and should be regarded only as a rough approximation.

^e Many of the area data are supplied for spin doublets for 3p and 4d because of the considerable width of many of those lines. Data for combined spin doublets in the 2p series for transition metals and the 3d for the rare earths are supplied because of the prevalence of shakeup lines, which makes it desirable to deal with the doublet as a whole.

from the ratios: $2p/2p_{3/2} = 3/2$, $3d/3d_{5/2} = 5/3$ and $4f/4f_{7/2} = 7/4$.

Peak height factors for the strong lines

Observations of the widths of the strong lines disclose that they are quite uniform. The height sensitivity fac-

tors were therefore derived from the area sensitivity factors, with suitable convolution of the unresolved spin doublets. For this it was assumed that the lines were 3.1 eV wide, found to be typical for these lines from insulating materials at a pass energy of 100 eV (PHI 550). This is the typical setting for survey spectra and for multiplexed (narrow scan spectra) used for quantitative work with the PHI 550 instrument.

Slight modifications in the assumption of equal line widths were made for the higher Z members of each series, e.g. Mg1s, Ge2p_{3/2}, As2p_{3/2}, Cs3d_{5/2} and Ba3d_{5/2}. Actual increments in line width of a few tenths of an eV over those of lower Z were noted in practice and used to correct the calculated peak heights for these elements, as indicated by the disparity from area sensitivity factors.

Values for the first series of transition elements are indicated in parentheses in Table 3, to indicate great variability with chemical state. These values are suggested for the diamagnetic states; most paramagnetic ones will have lower values. No values are given for the rare earths. The variability here is still more extreme, from the same effects—multiplet splitting and multi-electron processes.

Theoretical sensitivity factors for the secondary lines

The lines second in intensity are the 2s, 3p_{3/2}, 4d_{5/2} and 5d_{5/2} lines. Cross-sections for these transitions differ from those of the strong lines in that the curves $\ln(\sigma/\sigma_{F1s})$ vs. $\ln BE$ for Al X-ray photons have higher magnitude than those for Mg, and the curves diverge going to higher Z or higher binding energy (Fig. 7). The curves for the 2s lines between F and Sc are virtually straight, with correlation coefficient 0.9997. Those for 3p_{3/2} between Cu and Sn are straight segments with correlation coefficient 0.9998. Below Cu the curves have sharply higher slope. The 4d curves are unusual, composed of straight line segments Sb–La and Pt–U, with correlation coefficients 0.9985 and 0.9996 respectively. Values for the elements Hf–Ir lie close to the latter curve. The rare earths, between the two seg-

ments, form a transition region. The 4d lines of the first series, Sb–La, are very narrow. In the rare earths, changes in the energy relationships of the orbitals as the 4f shell becomes populated permit Coster–Kronig transitions involving the 4d electrons, the lifetime of the 4d ion becomes shorter, and the lines much wider, so that peak widths of the second series are some 2 eV wider than the first. Data for the 5d_{5/2} transition from Tl to Am form three straight line segments on the log–log plot, with that for Al X-rays some 15% larger in magnitude than that for the Mg X-rays.

Theoretical area sensitivity factors can be calculated for the secondary lines in the same fashion as for the strong lines, by applying energy correction factors to the cross-section curves. This has been done in Fig. 7 for the average of the cross-sections for Al and Mg X-rays. Since the relative cross-sections for Al X-rays are clearly larger than those for Mg X-rays, and the energy correction makes the disparity still larger, one should expect sensitivity factors for secondary lines relative to F1s with Al X-rays to be significantly larger than those by Mg X-rays, by 10–20%.

Empirical area sensitivity factors for the secondary lines

Factors were not ordinarily obtained directly from fluorides and potassium salts, but were derived from the sensitivity factors of the strong lines by multiplying by the area ratios of the secondary lines to the strong lines. Thus,

$$\frac{S_s}{S_p} = \frac{A_s}{A_p} \quad \text{and} \quad S_s = \frac{A_s}{A_p} (S_p) \quad (8)$$

where S is the sensitivity factor, A is the peak area, sub s refers to a secondary line, and sub p refers to a strong (primary) line. For example, the measured ratios of the 2s/2p_{3/2} peaks for magnesium in seven different magnesium compounds²¹ were multiplied by the derived area sensitivity factor for Mg2p_{3/2} (Table 3) of 0.079 to provide seven different empirical values for

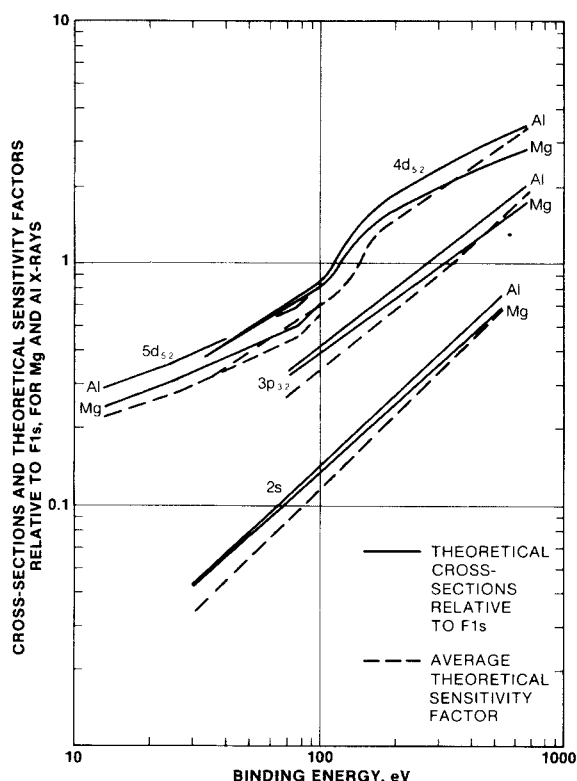


Figure 7. Photoelectric cross-sections of the secondary lines, plotted against binding energy of the transitions; derived theoretical sensitivity factors.

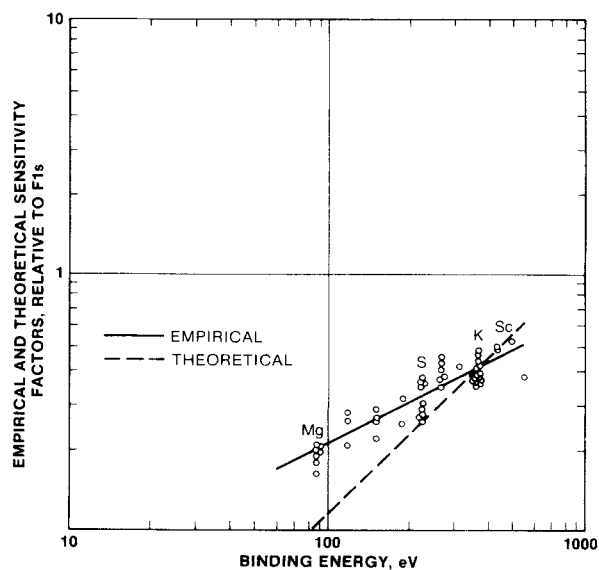


Figure 8. Empirical sensitivity factors for 2s transitions.

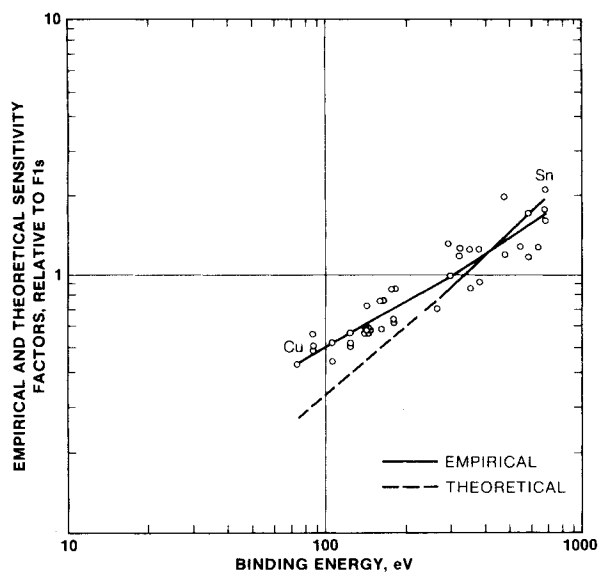


Figure 9. Empirical sensitivity factors for $3p_{3/2}$ transitions.

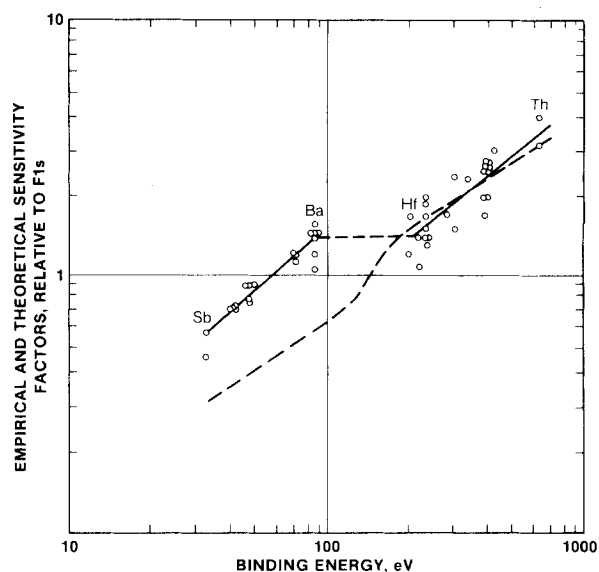


Figure 10. Empirical sensitivity factors for $4d_{5/2}$ transitions.

Mg2s. This was done for many compounds of the elements Mg–Ti, with data derived from Ref. 21. The data, plotted vs binding energy on a log–log plot, are shown in Fig. 8. Data²¹ for the $3p_{3/2}/3d_{5/2}$ ratio for elements Cu–Sn were treated similarly, multiplying by the $3d_{5/2}$

sensitivity factors. To these were added some data acquired since (Table 4) for both $3p_{3/2}/2p_{3/2}$ ratios and $3p_{3/2}/3d_{5/2}$ ratios. These supplied the data points for Fig. 9.

Data for one segment of the 4d curve, Fig. 10, points Sb–Ba, were generated from $4d/3d_{5/2}$ peak ratios in

Table 4. Area ratios used in deriving sensitivity factors for the secondary lines. (area ratios not cited in Ref. 21)

	Compound	X-Rays	2s/2p _{3/2}		Compound	X-rays	4d _{5/2} /3d _{5/2}	
Sc	Sc ₂ O ₃	Al	0.52	4 1317	Ba	BaF ₂	Mg	0.204
				4 1318		BaF ₂	Al	0.19
Cu	CuCN	Mg	0.168	4 1319		BaF ₂	Al	0.145
			3p _{3/2} /2p _{3/2}	4 1320		BaSO ₄	Al	0.18
Zn	ZnO	Al	0.126	4 1321		Ba Erucate	Al	0.19
				4 1322		Ba Chloranilate	Al	0.19
	ZnF ₂	Mg	0.109	4 1323	La	LaF ₃	Mg	0.24
				4 1324				
Ge	GeO ₂	Al	0.100					
As	As ₂ O ₃	Al	0.115	4 1325	Ir	Na ₂ IrCl ₆ · 6H ₂ O	Al	4d _{5/2} /4f _{7/2} 0.77
			0.094	4 1326			Bi	NaBiO ₃
			3p _{3/2} /3d _{5/2}	4 1327	Th	ThF ₄	Mg	0.43
Sr	SrF ₂	Mg	0.83	4 1328		ThF ₄	Al	0.55
Ag	AgOCCCF ₃	Al	0.42	4 1329				5d/4f _{7/2}
In	InF ₃	Al	0.33	4 1330	Th	ThF ₄	Mg	0.20
Sn	SnO	Al	0.38			ThF ₄	Al	0.225
	SnO ₂	Al	0.42	4 1331				
	NaSnF ₃	Al	0.50					
			4d/3d _{5/2}					
Sb	Sb ₂ S ₅	Al	0.21					
			0.17					
Te	KSbF ₆	Al	0.24					
			0.23					
	(NH ₄) ₂ TeO ₄	Al	0.26					
			0.23					
I	NaI	Mg	0.26					
			0.26					
	KI	Al	0.26					
			0.22					
	KIO ₄	Al						
			4d _{5/2} /3d _{5/2}					
Cs	CsOH	Al	0.175					
	CsCl	Al	0.16					
	Cs ₂ SO ₄	Al	0.175					

Table 4, multiplying by the sensitivity factors for $3d_{5/2}$. Similarly, peak area ratios in Ref. 21 for $4d_{5/2}/4f_{7/2}$ for elements Hf–Th were multiplied by area sensitivity factors for $4f_{7/2}$ to give data for the second segment.

As with the strong lines, the theoretical sensitivity factor curves were calculated from the average relative cross-sections for Mg and Al X-rays by applying energy corrections. Best fit straight lines were then calculated for the following segments:

Line	Elements	Correlation coefficients
2s	Mg–Ti	1.000
$3p_{3/2}$	Cu–Sn	0.999
$4d_{5/2}$	Sb–La	0.999
$4d_{5/2}$	Lu–U	1.000

Deviations of the theoretical $\ln S$ from these line segments were calculated, and subtracted from the appropriate $\ln S$ data for each element. The corrected $\ln S$ were fitted by a best straight line over the segments (2s) Mg–Ti, ($3p_{3/2}$) Cu–Sn, ($4d_{5/2}$) Sb–Ba and ($4d_{5/2}$) Hf–U. The intercepts at each elemental binding energy were calculated and the deviations $\ln S$ added back to give the points recorded in Table 3 and plotted in Figs. 8–10.

It will be noted that the level of the low *BE* segment of the $4d_{5/2}$ curve is very much higher than the theoretical curve, so that the value for Ba, element 56, is about the same as Hf, element 72. This poses a problem of drawing a reasonable transition curve for the rare earths. The dashed line shown in Fig. 10 is drawn in the absence of adequate knowledge about sensitivity factors of these elements.

Very few data for $5d_{5/2}$ lines were available, some from Ref. 21 and a few from Table 4. Values of the $5d_{5/2}/4f_{7/2}$ ratio were nearly constant, ranging from 0.16 for Pb to 0.13 for Th. These ratios were multiplied by the area sensitivity factors for $4f_{7/2}$ to give the few data points plotted in Fig. 11. A curve drawn through the points similar in shape to the theoretical one provided the data in Table 3.

Data for the 2s lines can be extended to lower *Z* elements if one uses relative area data for 2s/1s lines

and multiplies by the 1s sensitivity factor. When this was done for Na, the resulting value for the 2s sensitivity factor, based upon data from 33 compounds, was 0.13, considerably below the value of 0.17 calculated by extrapolation from the curve in Fig. 8. Data from very few oxides and fluorides place the 2s sensitivity factors at about 0.025 and 0.040 respectively, far below the extrapolated empirical curve, and rather close to the theoretical curve, which is nearly a straight line extended to these elements. Accordingly, in Table 3, are placed these values, with confidence in the value for Na, and considerably less confidence in the values for O and F.

The area sensitivity factors for the secondary lines in Table 3 are derived from 183 peak area ratios in Ref. 21 and Table 4, of which 63 were recorded using Mg X-rays and 120 were recorded using Al X-rays. The data were assembled without respect to the X-rays used. Examination of the data where both Mg and Al X-rays were used on compounds of the same element discloses that area ratios and derived sensitivity factors from Mg X-rays were above the median in one-fourth of the cases, below in three-fourths. This result is in agreement with the fact that the theoretical sensitivity factors for Al X-rays are larger than those for Mg X-rays in Figs. 8–11 by 10–20%.

Empirical height sensitivity factors for secondary lines

The secondary lines have varied line widths, and the task of deriving peak height sensitivity factors is more complex than that for the strong lines. For the 2s series the lines have significant extra width beginning with Mg2s. For O through Na, the area sensitivity values were used because the 2s lines were as narrow as the 1s lines (including F1s). For the series Mg–Sc, peak height ratios $2s/2p$ or $2s/2p_{3/2}$ were measured for about 60 compounds of these elements on two instruments at 100 eV pass energy. These ratios were plotted versus *Z*, and the best composite curve drawn through the points. Intercepts for each element were then multiplied by the $2p_{3/2}$ height sensitivity factors in Table 3. The results were added to Table 3.

For the 3p series, the procedure was similar, done in two segments. For the series Ti–As, observed peak height ratios $3p_{3/2}/2p_{3/2}$ (or $3p/2p_{3/2}$ when unresolved) were plotted vs *Z*, and the best monotonic curve drawn through the points. The value ranged from 0.14 for Ti to 0.06 for As. Intercepts at each *Z* were multiplied by peak height sensitivity factors for $2p_{3/2}$ to generate the factors in 3p or $3p_{3/2}$. The process was repeated for the $3p_{3/2}/3d_{5/2}$ ratio for elements Ga–Sn, multiplying by the $3d_{5/2}$ value. Some adjustment was required in the overlapping Ga–As region to make a single smooth curve (values in Table 3).

With the first $4d$ series, Sb–La, it was found that the ratio $4d/3d_{5/2}$ approximated 0.18, with no trend with *Z*. This was multiplied by the peak height sensitivity factors for $3d_{5/2}$ to give the $4d$ series in Table 3. For the second segment, Hf–Th, the same procedure was followed with the peak height ratio, $4d_{5/2}/4f_{7/2}$. This gave a monotonic curve, decreasing from 0.5 for Hf to 0.17 for Th. Intercepts at each *Z* multiplied by the $4f_{7/2}$ height sensitivity factors gave the values in Table 3. The peak height sensitivity factors for the intervening rare

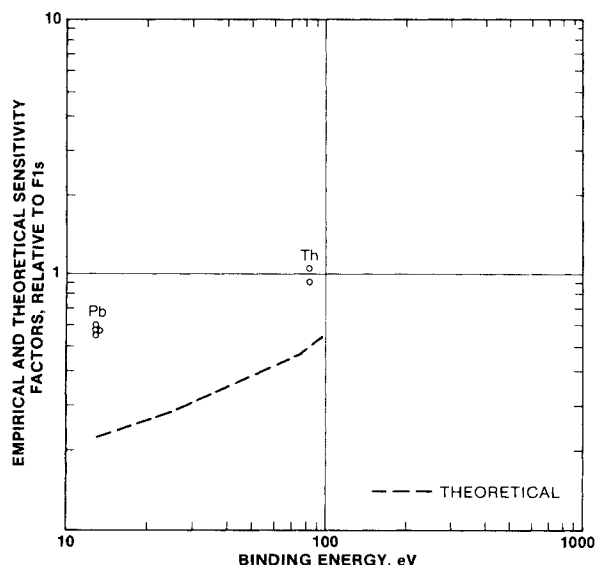


Figure 11. Empirical sensitivity factors for $5d_{5/2}$ transitions.

earths are left blank, because of their extreme variability with chemical state due to multiplet splitting and multi-electron processes.

Data for the 5d elements are confined to three elements—Pb, Bi and Th. The 5d/4f_{7/2} height ratio was constant at 0.13. This is in good agreement with the area ratios, as it should be, since the lines are narrow and equal to the width of the 4f_{7/2} lines.

In deriving these data on height factors for the secondary lines, peak height ratios for some 194 compound entries were used. Of these, 133 were based upon Mg radiation. Of these, 84, or 63% of the values were below the representative curve chosen. This selectivity factor further corroborates the theoretical cross-section data that place energy corrected values for secondary lines for Mg X-rays some 10–20% below those for Al.

DISCUSSION

Figures 3–6 all demonstrate a consistent conclusion: The empirical sensitivity factors for the strong lines of most of the elements relative to F1s are considerably larger than those predicted from calculated cross-sections. Only the elements neighboring fluorine show reasonable agreement; the lower members of the 1s series, Li–C, are considerably too high, plus Mg–Sc in the 2p series, and all of the 3d and 4f series. The difference is roughly 25–40% (Fig. 12). It may be noted from Fig. 1 that the error would be considerably less if no energy correction had been made, and if the relative cross-sections themselves had been used. The concept is not valid of course—it merely means that the error in the cross-sections relative to F1s operates so that applying the logical energy correction makes the error worse. With some instruments¹⁰ the transmission apparently is less sensitive to kinetic energy, so the overall energy correction is minimal or unnecessary. It might be noted that it happens that F1s turns out to be a poor choice as a standard, and that use of K2p_{3/2} would have given better agreement of theory with experiment for all but F1s and its near neighbors in the 1s series.

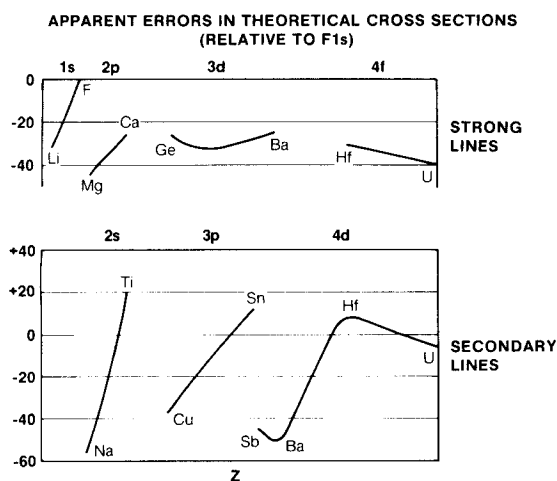


Figure 12. Apparent differences between empirical and theoretical sensitivity factors.

The conclusion that the relative cross-sections are seriously in error is supported by an earlier similar study by Evans, Pritchard and Thomas.¹⁴ They used an analyzer with different transmission function, and a smaller number of compounds. Their approach was exactly analogous, however, and they found similar disagreement with calculated cross-sections.

The analogy with their results extends further to the secondary lines as well (Fig. 12). We find the 2s empirical curve to be of much lower slope than the theoretical one, and to cross it at potassium. The 3p empirical curve is also of lower slope and crosses that theoretical one at about rhodium. The empirical 4d curve is in reasonable agreement with the higher *Z* segment, but in very poor agreement with the Sb–Ba segment. With the latter the slope of the empirical curve is higher and the absolute values are more than twice those predicted by theory. The few empirical points for the 5d series are 2–3 times higher than those from theory. All of these conclusions except that pertaining to the 5d are qualitatively similar to those reached by Evans *et al.*¹⁴

The effect of surface contamination

A thin contaminating layer attenuates intensities of electrons from beneath, according to

$$I/I_0 = e^{-d/\lambda_c} \quad (8)$$

where *d* is the thickness and λ_c the mean free path in the contaminating layer. The carbon line from the thin contaminating layer has an intensity

$$I_c = (n f \sigma \phi y A T \lambda_c) (1 - e^{-d/\lambda_c}) = I_{\infty} (1 - e^{-d/\lambda_c}) \quad (9)$$

where I_{∞} is the intensity of the carbon 1s line from an infinitely thick layer. For very thin layers when d/λ_c is less than c.0.2, the relation is close to

$$I_c = I_{\infty} (d/\lambda_c) \quad \text{or} \quad I_c/I_{\infty} = d/\lambda_c \quad (10)$$

Let us assume the same exponential relationship of λ_c and E_c as we have above

$$\lambda_c = k E_c^{0.66} \quad (11)$$

and, for Mg and Al X-rays respectively

$$\lambda_c = 93.53 k, 107.83 k \quad (12)$$

For two values of d/λ_c of 0.1 and 0.2, representing reasonable and probably maximum levels of contamination by adventitious hydrocarbon, the attenuation factor for any line of kinetic energy *E* is given by

	Mg X-rays	Al X-rays
$d/\lambda_c = 0.1$	$\exp(-9.353 E^{-0.66})$	$\exp(-10.783 E^{-0.66})$
$d/\lambda_c = 0.2$	$\exp(-18.706 E^{-0.66})$	$\exp(-21.566 E^{-0.66})$

With the F1s line as standard, the effect of contamination is not large, amounting to less than 10% for lines up to about 1000 eV binding energy. The effect is opposite to the combined energy dependent factors, *AT* and λ , for these instruments that scan the spectra by varying the retarding energy.

Comparison with other data on relative line areas

There have been other tabulations of sensitivity factors, and of cross-sections derived from sensitivity factors, some with similar or identical instruments and some with instruments of different transmission function. It is worthwhile to comment upon similarities and differences of this study with those studies in which measurement of peak areas in stoichiometric compounds were involved. Studies of relative line areas of metals are not included in the comparison, because of special problems associated with the asymmetric line shapes in their spectra.

Two round robin studies^{22,23} indicate very wide discrepancies in measurement by different laboratories of peak ratios for different elements in stoichiometric compounds, and even for two peaks for the same element. Many of these varying data were from identical instruments or instruments of similar transmission characteristics. An important feature of the measurements was that they were to be done in the normal operating mode for the laboratory. It is clear that many of the instruments in normal use are not adequately maintained, or calibration procedures are not well understood. Previous studies with single instruments¹ and the following comparisons indicate that reproducibility in area ratios in properly maintained instruments is far better than that indicated by the round robin studies.

In this study the data used in developing the area sensitivity factors for the strong lines do exhibit scatter from the derived curves. The average deviations from the derived sensitivity factors are 12%, 11%, 17% and 17% respectively, for the 1s, 2p, 3d and 4f series. Data for the secondary lines exhibit similar scatter. It is expected that area sensitivity factors are more useful than height sensitivity factors because of the variability in line width, due to multiple chemical states and differential charging.

Comparison with earlier study⁵

Some of the earlier data are included in the present broad tabulation. Those excluded are the data with Na1s as the secondary standard and those of the cyano complexes which have been shown to be unreliable. Comparison of the overall results in the earlier work with the more extensive data here discloses substantial agreement in the 1s series, except Mg1s; good agreement in the 2p series; values in the 3d series in the earlier work averaging 11% higher, with large 22% standard deviation, and values in the 4f series averaging 15% lower.

Comparison with Nefedov *et al.*^{8,9}

Experimental sensitivity factor data in those two articles, obtained with Al X-rays with the Varian instrument, are tabulated individually relative to the Na1s line as a primary standard. Their data from two fluorides, NaF and Na₂SiF₆, places Na1s at 1.88 relative to F1s. If we use this as a ratio, we can calculate their

sensitivity factors individually relative to F1s, and compare them with the smoothed factors derived here. They tabulate 41 elements of the first 56. These average 92% of the corresponding values herein, with a standard deviation of 12%. There are no substantial deviating trends; the most serious discrepancies are with Mg1s, and Zn2p_{3/2} and As2p_{3/2}, all low kinetic energy lines, where their values are below those reported here. With lines of very low kinetic energy it is expected that contamination of the surface will introduce greater variability in results.

Comparison with Jørgensen and Berthou^{6,7}

Very shortly after the first tabulation⁵ these authors published extensive data on relative peak heights, derived from data on more than 600 inorganic compounds, with both Mg and Al radiation using the Varian instrument. The exact method of treatment of the data was not disclosed, but the data were presented as peak height relative to F1s for individual elements, unsmoothed with *Z*. Data are compared here with present peak height sensitivity factors, that are shown in Table 3. Their data for I, Rb and for Mg X-rays U, are not included because they seem to be clearly anomalous. The agreement was reasonable for all but the 2s and 2p lines. The differences with X-ray energy for the secondary lines are not so evident as we might expect.

Comparison with Evans, Pritchard and Thomas¹⁴

Evans and co-workers tabulated line area ratios from a wide variety of compounds, using Mg X-radiation with the AEI instrument in the FRR mode. This instrument mode has a transmission varying with E^{+1} rather than E^{-1} . They made energy corrections assuming $\lambda \sim E^{0.5}$, included an average factor correcting for average contamination layer, and arrived at a set of empirically derived cross-sections, which were smoothed by a polynomial fit. They then compared these cross-sections with those calculated by Scofield¹⁵ in their Fig. 3. Broad conclusions were mentioned above. Conclusions in greater detail are the following (F1s is the standard):

- 1s Experimental values for Li are higher by roughly 50%. The rest of the elements, B–F, are close.
- 2p Eight elements, Na–Ca, are 25–35% above theory. The transition metals are below theory.
- 3d The six elements shown Br–I are all 25–40% above theory. No points are shown for Y–Pd.
- 4f The seven elements shown average about 15% above theory.
- 2s Seven elements form a curve of much lower slope than the theoretical, crossing at silicon.
- 3p The experimental curve follows the theoretical one rather well above the transition metals.
- 4d The segment Cd–Ba is clearly 10–100% above theoretical. That for W–Th seems to be somewhat below theory.

There is thus reasonable agreement in some detail with the conclusions of the present study.

Comparison with Castle and West¹⁰

Castle and West have published a similar set of data, relative to F1s, determined by area ratios, using a Vacuum Generators ESCA 3 Mk II instrument with Si K α X-rays and operating in the retarding mode. They have evidence that the transmission factor varies more like $E^{-0.5}$ rather than E^{-1} . From cross-section data it is expected that the sensitivity factors for the strong lines should be similar to the data for Mg and Al radiation: those for the secondary lines should be somewhat smaller.

Very good correspondence between their values and ours are reported for the 1s lines ($96 \pm 9\%$) and the 2p lines ($87 \pm 13\%$) and lower average values for the 3d lines ($82 \pm 13\%$). The 2s and 3p lines did not average to smaller values, as expected, but were more nearly the same as those reported herein, but with large scatter (standard deviation 26–27%).

Comparison with Szajman *et al.*²⁴

In a recent article Szajman, Jenkin, Leckey and Liesegang present experimentally derived photoelectric cross-sections for the subshells of Li, F, Na, Mg, Cl, K, Ca, Cr, Zn, Br, Rb, Sr, I, Cs, Ba and Pb. They used a spectrometer of similar transmission characteristics to the instruments used in this study. Results were qualitatively similar to those described herein; Relative to F1s, values were larger for Li1s, the 2p_{3/2} series and the 3d_{5/2} series. Those for 2s were higher than theory for the low *Z* members, and became lower above magnesium. Those for 4d_{5/2} were 13–31% higher than theory for I, Cs, Ba and 16% lower for Pb. Values for 4f_{7/2} and 5d_{5/2} levels of Pb were 11% and 54% high respectively. These discrepancies from theory are all in the same direction as those observed herein.

REFERENCES

1. C. D. Wagner, ASTM Special Publication 643, p. 31. American Society for Testing and Materials, Philadelphia, Pennsylvania (1978).
2. C. D. Wagner, L. E. Davis, and W. M. Riggs, *Surf. Interface Anal.* **2**, 53 (1980).
3. R. F. Reilman, A. Msezane and S. T. Manson, *J. Electron Spectrosc. Relat. Phenom.* **8**, 389 (1975).
4. O. A. Baschenko and V. I. Nefedov, *J. Electron Spectrosc. Relat. Phenom.* **17**, 405 (1979).
5. C. D. Wagner, *Anal. Chem.* **44**, 1050 (1972).
6. C. K. Jørgensen and H. Berthou, *Discuss. Faraday Soc.* **54**, 269 (1973).
7. H. Berthou and C. K. Jørgensen, *Anal. Chem.* **47**, 21 (1975).
8. V. I. Nefedov, N. P. Sergushin, J. M. Band and M. B. Trzhaskovskaya, *J. Electron Spectrosc. Relat. Phenom.* **2**, 383 (1973).
9. V. I. Nefedov, N. P. Sergushin, Y. V. Salyn, I. M. Band and M. B. Trzhaskovskaya, *J. Electron Spectrosc. Relat. Phenom.* **7**, 175 (1975).
10. J. E. Castle and R. H. West, *J. Electron Spectrosc. Relat. Phenom.* **19**, 409 (1980).
11. C. D. Wagner, W. M. Riggs, L. E. Davis, J. F. Moulder and G. E. Muilenberg, *Handbook of X-Ray Photoelectron Spectroscopy*, Perkin-Elmer Corporation, Physical Electronics Division, Eden Prairie, Minnesota (1979).
12. M. P. Seah, *Surf. Interface Anal.* **2**, 222 (1980).
13. B. Barbaray, J. P. Contour and G. Mouvier, *Analisis* **5**, 413 (1977).
14. S. Evans, R. G. Pritchard and J. M. Thomas, *J. Electron Spectrosc. Relat. Phenom.* **14**, 341 (1978).
15. J. H. Scofield, *J. Electron Spectrosc. Relat. Phenom.* **8**, 129 (1976).
16. R. S. Swingle, *Anal. Chem.* **47**, 21 (1975).
17. W. J. Carter, G. K. Schweitzer and T. A. Carlson, *J. Electron Spectrosc. Relat. Phenom.* **5**, 827 (1974).
18. P. W. Palmberg, *J. Vac. Sci. Technol.* **12**, 379 (1975).
19. C. J. Powell, *Surf. Sci.* **44**, 29 (1974).
20. D. R. Penn, *J. Electron Spectrosc. Relat. Phenom.* **9**, 29 (1976).
21. C. D. Wagner, *Anal. Chem.* **49**, 1282 (1977).
22. T. E. Madey, C. D. Wagner and A. Joshi, *J. Electron Spectrosc. Relat. Phenom.* **10**, 359 (1977).
23. C. J. Powell, N. E. Erickson and T. E. Madey, *J. Electron Spectrosc. Relat. Phenom.* **17**, 361 (1979).
24. J. Szajman, J. G. Jenkin, R. C. G. Leckey and J. Liesegang, *J. Electron Spectrosc. Relat. Phenom.* **19**, 383 (1980).

Received 13 April 1981; accepted 23 June 1981

© Heyden & Son Ltd, 1981